Vol. 122 (2012) ACTA PHYSICA POLONICA A No. 3

Proceedings of the 12th International Symposium on Physics of Materials, Prague, September 4–8, 2011

Synthesis and Luminescent Properties of Eu^{3+} Doped Crystalline Diphosphate $Na_2ZnP_2O_7$

L. GUERBOUS[a,*] AND L. GACEM[b]

[a]Laser Department/Nuclear Research Center of Algiers, 2 Bd., Frantz Fanon, BP 399, Alger, Algeria

[b]Materials Science Department, Faculty of Science, University of Djelfa, Algeria

Undoped and Eu^{3+}-doped disodium zinc diphosphate $Na_2ZnP_2O_7$ (NZPO) single crystals are grown by the Czochralski method. X-ray diffraction, Fourier transform infrared and Raman techniques were used to check the crystallographic structure. Excitation and emission spectra were measured at room temperature and studied. The Eu^{3+} ions occupy a non-centrosymmetric site with different coordination number. Very efficient energy transfer from O–Eu^{3+} band state to Eu^{3+} excited energy levels is highlighted.

PACS: 78.20.−e, 78.55.−m, 78.55.Hx

1. Introduction

Wide band gap inorganic materials (oxides, fluorides, sulfides, phosphates, etc.), actived by rare-earth ion elements are widely and extensively investigated and used in several applications, such as optical amplification, lasing, optical data storage, upconversion, VUV phosphors, gamma and X-ray scintillators [1–6]. Because of the extraordinary versatility of phosphate structures which facilitates the design of new compounds with appropriate optical properties, they have gained much more attention of several researchers. Furthermore, the properties of these inorganic materials are strongly dependent on doping ions, their concentration, charge and the symmetry of local environment.

Many phosphate materials have been studied as a host of rare-earth ions. Indeed, the luminescence properties of various lanthanide dopants phosphates compounds with the formulation $AREP_4O_{12}$ (A = Cs, Rb, K, Na, Li and RE = La, Pr, Gd, Y), which form a family of related polyphosphate compounds, have been reported [7]. However, very few references are available concerning the luminescence of rare-earth ions doped mixed diphosphates with the general formula $A_2MP_2O_7$ (A = Na, K and M = Co, Cu, Zn). These materials exhibit the melilite structure type and indexed in the tetragonal system [8–12]. Among these inorganic materials, the disodium zinc diphosphate $Na_2ZnP_2O_7$ (called NZPO) can be synthesized as a glass or a crystallized compound. Several dopings and/or substitution can be made for both shaping and this study reports on the case of Eu^{3+} doped NZPO single crystal. $Na_2ZnP_2O_7$ diphosphate material has been doped with Co^{2+} [10], Ag^{+} [13], Mn^{2+} [14] ions and by Eu^{3+} by [15]. Europium activated inorganic materials have been studied intensely, since Eu^{3+} is an ideal red-emitting activator and Eu^{2+} can emit photons in a wide energy range from UV to red, depending on the 5*d* level position which depends on the nature of the host [16]. Furthermore, for a very large number of applications, Eu^{3+} ions are used as luminescent centre in phosphor display, imaging. To obtain an efficient inorganic material for such application we must be able to tune, in some extent, the luminescence properties of these materials to match the applications. Better understanding of absorption and luminescence mechanisms in correlation with the nature of the host lattices is the good way to do.

We report in this paper the single crystals growth of undoped and 1% Eu^{3+}-doped $Na_2ZnP_2O_7$ diphosphate. We present the structural analysis by X-ray diffraction (XRD), Fourier transform infrared (FTIR), and Raman techniques of the samples. We report the absorption, excitation and emission spectra and their investigation.

2. Experimental procedure

2.1. Powder preparation

Pure $Na_2ZnP_2O_7$ and 1% Eu^{3+}-doped compounds were synthesized by the conventional solid state phase reaction method. Stoichiometric mixture of high purity $NH_4H_2PO_4$, Na_2CO_3 and ZnO (or $NaPO_3$, ZnO) powders were carefully ground together in an agate mortar, and progressively heated in a platinum crucible up to 350 °C to allow ammonia and water to evacuate. After grinding, the powders were heated at 720 °C and maintained at this temperature during 2 days for departure of carbon dioxide in order to complete the reaction, and then the product is melted at 820 °C. The 1% europium trivalent doping is accomplished by adding the adequate amount of Eu_2O_3 in starting materials.

2.2. Single-crystal growth

$Na_2ZnP_2O_7$ melts congruently at 796 °C. Pure and Eu^{3+}-doped single crystals were grown by using the Czochralski pulling method. The following conditions are used to grow the crystal. The synthesized compound was placed in a Pt-crucible of 35/40 mm diameter/height and inductively heated in air to a temperature of 30 °C

---

[*] corresponding author; e-mail: `guerbous@yahoo.fr`

higher than the crystallization temperature, for about 3 h in order to melt completely and homogeneously. During crystal growth, in the absence of a seed crystal, a Pt rod is rotated and withdrawn at a speed of 20 rpm and 0.5–1 mm/h, respectively. Preferential cleavage plane is perpendicular to the growth direction and corresponds to (001) plane. Photograph of cleaved single crystal sample is shown in Fig. 1. Powder samples used in this study, for luminescence measurements, are crushed from crystals.

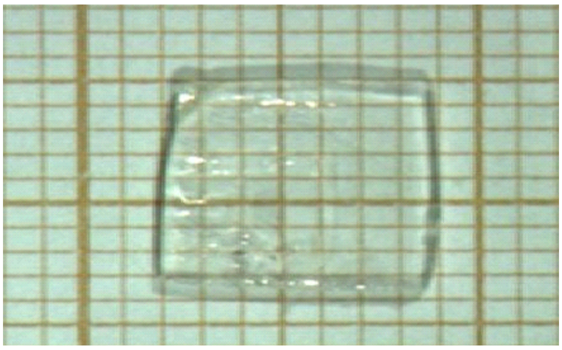

Fig. 1. Platelet of NZPO:Eu^{3+} single crystal oriented along c direction, $d = 1.6$ mm, prepared using the Czochralski method.

2.3. Characterization techniques

Phase structure of crystalline powders was controlled by analyzing the diffraction spectra. XRD experiments were performed on a Philips PW1820 X-ray diffractometer, with Cu K_α radiation ($\lambda = 1.5406$ Å). The data were collected using a Ni-filtered Cu-target tube. FTIR spectroscopy was performed using a Bruker IFS113V FTIR instrument over the range 4000–200 cm^{-1} with 2 cm^{-1} resolution. Sixteen scans were obtained at 2.0 cm^{-1} increment. The samples were prepared as KBr disks from the ground powder of selected crystals. The Raman spectrum of crystal sample was recorded with a micro-Raman XY Dilor instrument in backscattering geometry at room temperature. Room temperature absorption spectra were recorded on a Varian Cary 5000 spectrophotometer in an allowed wavelength range of 175–3300 nm. Excitation and emission spectra were recorded on powder samples (crushed from single crystal) at room temperature. The luminescence properties were studied using a SPEX Jobin Yvon spectrofluorimeter Fluorolog 2 system.

3. Results and discussion

3.1. Structural characterization

3.1.1. XRD analysis

The XRD results (Fig. 2) of undoped and Eu^{3+}-doped $Na_2ZnP_2O_7$ single crystals are in a good agreement with the standard data ICSD #95958, and indicate clearly that our samples exhibit a single phase. The structural parameters $a = 7.685$ Å, $c = 10.265$ Å are close to those previously reported in the literature by Majling et al. [17] $a = 7.692$ Å, $c = 10.273$ Å, in the crystal structure described by Erragh et al. [12] $a = 7.656$ Å, $c = 10.233$ Å and also reported by Belharouak et al. [13] $a = 7.685$ Å, $c = 10.265$ Å.

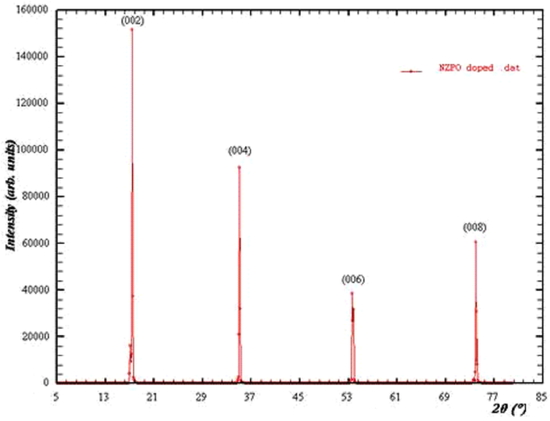

Fig. 2. X-ray diffraction pattern of undoped and Eu^{3+}-doped $Na_2ZnP_2O_7$ single crystals.

More detailed analysis of the $Na_2ZnP_2O_7$ single crystal structure was performed by Belharouak et al. [11] using X-ray technique, in which a new model explaining the actual large unit cell ($a = b = 2177.1(3)$ pm, $c = 1028.5(2)$ pm, $Z = 32$) was determined. The structure was made up of $[ZnP_2O_7]$ layers consisting of corners sharing $[P_2O_7]$ groups and isolated $[ZnO_4]$ tetrahedra, the sodium atoms are located between the layers in 7- or 8-fold coordinated sites. This description shows that $Na_2ZnP_2O_7$ has a very complex structure and leads even in a single crystal for both sodium and zinc ions to several non-equivalent positions existence (8 and 6, respectively) [14]. Using ESR analysis and the fluorescence measurement of Mn^{2+} doped $Na_2ZnP_2O_7$ single crystal, Gacem et al. [14] have shown that the Mn^{2+} ions are substituted for both Zn^{2+} and Na^+ ions, decreasing the concentration of octahedral sites for manganese. Because the peak positions of the doped $Na_2ZnP_2O_7$ are similar to the pure sample, it is clear that doping with Eu^{3+} does not change general structure of the host material. According to the XRD phase analyzed and the charge balance rule, Eu^{3+} cations are expected most probably to be substituting for the Na^+ cations in the $Na_2ZnP_2O_7$ host lattice. We think that the electrical neutrality can be done by the presence of gaps on sites sodium.

3.1.2. FTIR and Raman spectroscopy

Important informations of the symmetry P_2O_7 group in $Na_2ZnP_2O_7$ material structure can be provided by FTIR and Raman spectra (Fig. 3a, b). The FTIR and Raman spectra show a number of broad absorptions and peaks particularly in the range 1188–462 cm^{-1}. The vibrational frequencies of PO_3 are expected to be higher than those for P–O–P groups because of the strength of bond in the PO_3 group compared to that in the P–O–P bridge. Based on the literature [18–21], the frequencies of the $P_2O_7^{4-}$ anions are assigned to the vibration of the

PO_3 groups and P–O–P bridge and they are listed in Table. The values of the frequencies in Table allow us to confirm the local symmetry of P_2O_7 group in $Na_2ZnP_2O_7$ diphosphate structure.

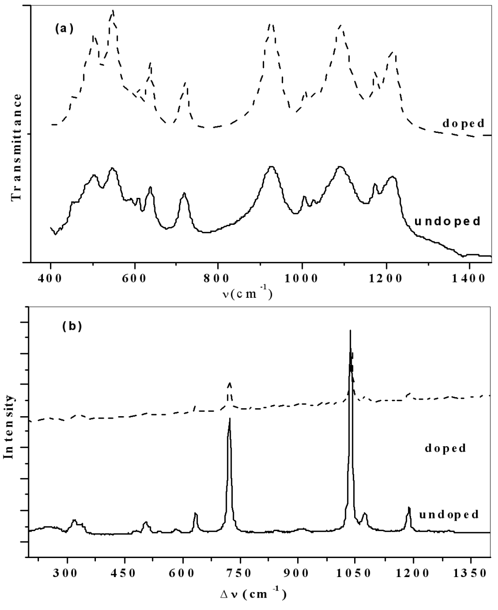

Fig. 3. (a) FTIR and (b) Raman spectra of undoped and Eu^{3+}-doped $Na_2ZnP_2O_7$.

3.2. Steady photoluminescence spectra, excitation and emission spectra

Room temperature emission spectrum of Eu^{3+} in $Na_2ZnP_2O_7$ diphosphate consists of numerous narrow lines resulting from the ${}^5D_0 \to {}^7F_{0-4}$ transitions under UV excitation (220 nm) (Fig. 4). The transition selection rules are completely lifted. The ${}^5D_0 \to {}^7F_0$ transition was observed as anticipated by the single Eu^{3+} site present in the crystal structure. The ${}^5D_0 \to {}^7F_2$ lines displaying peaks in the 610 nm region which dominates in intensity relative to the ${}^5D_0 \to {}^7F_1$ indicating that Eu^{3+} occupies a crystallographic site with no inversion symmetry. This result is in contradiction with that observed by Erragh et al. [15] in which they have observed that in the same material the emission spectrum shows a dominate ${}^5D_0 \to {}^7F_1$ which indicates the centrosymmetric site for Eu^{3+}.

TABLE

The infrared frequencies assignment (in cm^{-1}) for $Na_2ZnP_2O_7$ diphosphate.

IR	Raman	Attribution
	1188	$\nu_{as}(PO_3)$
1184		$\nu_{as}(PO_3)$
1149		$\nu_{as}(PO_3)$
	1075	$\nu_s(PO_3)$
	1038	$\nu_s(PO_3)$
1034		$\nu_s(POP)$
1016		$\nu_s(PO_3)$
983		$\nu_s(PO_3)$
	917	$\nu_{as}(POP)$
	844	$\nu_{as}(POP)$
767		$\nu_{as}(POP)$
	723	valence: $\nu_s(POP)$
677		$\nu_s(POP)$
	635	$\nu_s(POP)$
619		$\delta_{as}PO_3$
600		$\delta_{as}PO_3$
	583	$\delta_s(PO_3)$
580		deformation: $\delta_s(PO_3)$
	542	$\delta_{as}(PO_3)$
522		$\delta_{as}(PO_3)$, $\delta_s(PO_3)$
	505	$\delta_{as}(PO_3)$, $\delta_s(PO_3)$
462		$\delta_{as}(PO_3)$
	340	external modes
	318	external modes

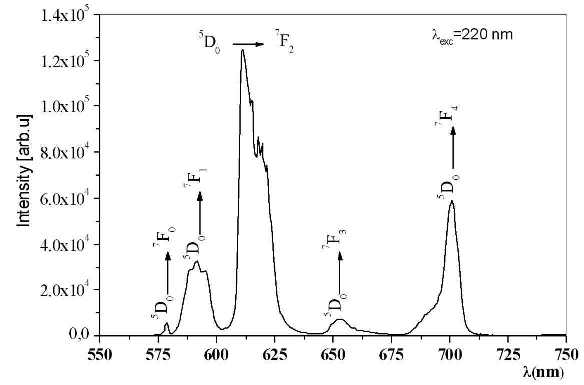

Fig. 4. Room temperature emission spectrum of $Na_2ZnP_2O_7:Eu^{3+}$, under the 220 nm excitation wavelength.

Furthermore, the inhomogeneous broadening of the emission peaks indicates that the Eu^{3+} ion occupies sites with different coordination number. The excitation spectra were measured at room temperature monitoring the ${}^5D_0 \to {}^7F_2$ transitions at 610 nm. The spectra consisted of sharp lines due to the transitions from ${}^7F_0$ ground level to the ${}^{2S+1}L_J$ excited levels of Eu^{3+} as well as the wide charge transfer transition at around 220 nm (34354 cm^{-1}, 5.63 eV) (Fig. 5) which is in good agreement with that found by Yuang et al. [16]. The position of the charge transfer transition energy is observed also by the room temperature absorption spectrum of Eu^{3+} in $Na_2ZnP_2O_7$ shown in the same figure.

From the excitation and emission spectra, we attempt to construct the schematic configurational coordination energy level diagram of the Eu^{3+} ion incorporated NZPO material (Fig. 6). This schematic shows the ground (${}^7F_J$), emitting (${}^5D_J$) and O^{2-}–Eu^{3+} charge transfer state. The shifted parabola shows qualitatively the po-

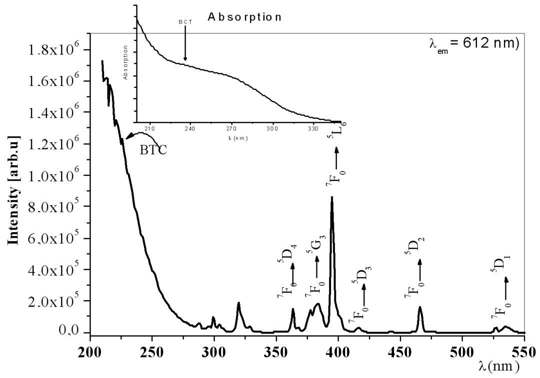

Fig. 5. Room temperature excitation spectrum of $Na_2ZnP_2O_7:Eu^{3+}$ monitoring 612 nm emission wavelength ($^5D_0 \to {}^7F_2$ transition). Room absorption spectrum of $Na_2ZnP_2O_7:Eu^{3+}$ is shown in the inset.

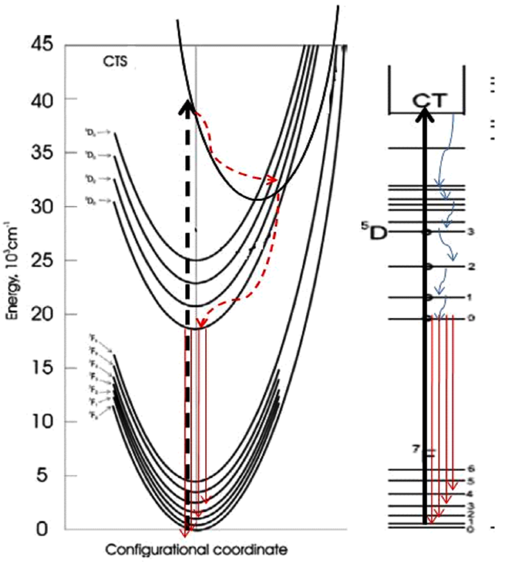

Fig. 6. Configuration coordinate diagram for the $4f$ and the lowest charge transfer state (CTS) (right side). Energy level diagram (left side) of Eu^{3+}-doped $Na_2ZnP_2O_7$, illustrating sequential quenching of ^5D emissions.

sition of the O^{2-}–Eu^{3+} state, which feeds the emitting (^5D_J) levels. Only a few parabolas of the $4f^6$ configuration have been drawn.

4. Conclusion

Undoped and 1% Eu^{3+}-doped disodium zinc diphosphate $Na_2ZnP_2O_7$ (NZPO) single crystals are synthesized by means of the Czochralski method. Crystallographic structure has been checked by XRD, FTIR and Raman spectra. Room temperature emission and excitation spectra were measured and investigated. The emission spectrum analyzes shows that Eu^{3+} ions occupy non--centrosymmetric sites with different coordination number. The charge transfer band transition between the top of valence band and europium ions has been observed at 220 nm (34354 cm^{-1}, 5.63 eV). The energy transfer phenomenon in NZPO:Eu^{3+} system is interpreted on the basis of a resonance crossover between the O–Eu^{3+} band state and the ^5D_J levels.

References

[1] D.W. Hewak, *Curr. Opin. Solid State Mater. Sci.* **5**, 469 (2001).

[2] D. Ehrt, *J. Non-Cryst. Solids* **348**, 22 (2004).

[3] J.S. Neal, L.A. Boatner, D. Wisniewski, J.O. Ramey, *Proc. SPIE* **6706**, 670618 (2007).

[4] G. Blasse, B.C. Grabmaier, *Luminescent Materials*, Springer-Verlag, Berlin 1994.

[5] M.T. Averbuch-Pouchot, A. Durif, in: *Topics in Phosphate Chemistry*, World Scientific Press, Singapore 1996.

[6] L. Guerbous, O. Krachni, *J. Mod. Opt.* **53**, 2043 (2006).

[7] P. Dorenbos, T. Shalapska, G. Stryganyuk, A. Gektin, A. Voloshinovskii, *J. Lumin.* **131**, 633 (2011).

[8] M. Kimata, *Neues Jahr B. Miner.* **146**, 221 (1983).

[9] K. Hagiya, M. Ohmasa, K. Iishi, *Acta Crystallogr. B* **49**, 172 (1993).

[10] L. Beaury, *J. Solid State. Chem.* **177**, 1437 (2004).

[11] I. Belharouak, P. Gravereau, C. Parent, J.P. Chaminade, E. Lebraud, G. Le Flem, *J. Solid State Chem.* **152**, 466 (2000).

[12] F. Erragh, A. Boukhari, B. El Ouadi, E.M. Holt, *J. Crystallogr. Spectrosc. Res.* **21**, 321 (1991).

[13] I. Belharouak, C. Parent, P. Gravereau, J.P. Chaminade, G. Le Flem, B. Moine, *J. Solid State Chem.* **149**, 283 (2000).

[14] L. Gacem, A. Artemenko, D. Ouadjaout, J.P. Chaminade, A. Garcia, M. Pollet, O. Viraphong, *Solid State Sci.* **11**, 1854 (2009).

[15] F. Erragh, A. Boukhari, A. Sadel, E.M. Holt, *Acta Crystallogr. C* **54**, 1373 (1998).

[16] J.-L. Yuang, X.-Y. Zeng, J.-T. Zhao, Z.-J. Zhang, H.-H. Chen, G.-B. Zhang, *J. Solid State Chem.* **180**, 3310 (2007).

[17] J. Majling, S. Palco, F. Hanic, J. Petrovic, *Chem. Zvesti.* **28**, 294 (1974).

[18] V.P. Mahadevan Pillai, B.R. Thomas, V.U. Nayer, Kwang-hwa Lii, *Spectrochim. Acta A* **55**, 1809 (1999).

[19] V. Vincent, C. Breandon, G. Nihol, J.-R. Gavarri, *Eur. J. Solid State Inorg.* **34**, 571 (1997).

[20] N. Khay, A. Ennaciri, M. Harcharros, *Vibrat. Spectrosc.* **27**, 119 (2001).

[21] M. Férid, K. Harchani-Naifer, *Mater. Res. Bull.* **39**, 2209 (2004).